

# Hydrophilic polymer nanofibre networks for rapid removal of aromatic compounds from water†

Mohan Raj Krishnan,<sup>a</sup> Sadaki Samitsu,<sup>\*a</sup> Yoshihisa Fujii<sup>a</sup> and Izumi Ichinose<sup>\*ab</sup>

Cite this: *Chem. Commun.*, 2014, 50, 9393

Received 10th March 2014,  
Accepted 4th July 2014

DOI: 10.1039/c4cc01786b

www.rsc.org/chemcomm

**Hydrophobic mesoporous polymer nanofibre networks were converted to hydrophilic ones by a mild sulfonation reaction. The resultant mesoporous polystyrene with a large free surface area effectively captured water-soluble dye molecules and allowed aromatic compounds to rapidly permeate into the internal binding sites.**

Precise fabrication of nanoporous polymers is indispensable for functional improvement of adsorbents.<sup>1</sup> Control of molecular diffusion in nanopores also has an important effect on their performance in applications such as separation membranes, humidity conditioning, and drug release. The fabrication of molecular-scale pores has been one of the main targets in the field of coordination/crosslinked polymers.<sup>2–4</sup> Relatively large meso- and macro-pores have been produced by phase separation of block copolymers,<sup>5–9</sup> supercritical carbon dioxide foaming,<sup>10,11</sup> and freezing techniques,<sup>12–14</sup> as well as by conventional phase separation methods.<sup>15,16</sup> However, mesoporous materials are not easily obtained from common polymers, which have generally non-crystalline features. This is because the mesopores formed in glassy polymers are readily extinguished by strong Laplace force.<sup>8</sup> In particular, in the phase separation process, the large diffusion length of solvent molecules can result in the formation of macroporous structures. Therefore, mesoporous materials with sharp pore size distributions and large specific surface areas have not been produced to a significant extent from common polymers.

Very recently, we reported a flash freezing route to the fabrication of mesoporous nanofibre networks of engineering polymers.<sup>17</sup> This method is based on nanocrystallization of solvent molecules under deep-frozen conditions and subsequent spatially restricted phase separation. The resulting mesoporous

polymers with large free surface areas would be ideal adsorbents for oil-contaminated water if the hydrophobic mesopores could be converted to hydrophilic ones. In this paper, we report controlled sulfonation of the inner surfaces of the mesopores and significant rapid adsorption of organic compounds from water.

Polymer nanofibre networks were prepared from solutions of polystyrene (PS), polysulfone, polyethersulfone, polycarbonate poly(*p*-phenylene oxide), and polyetherimide by a reported method (see ESI†).<sup>17</sup> For example, a 20 wt% dimethylformamide (DMF) solution of PS was applied as a coating to the inner surface of a glass bottle and immersed into liquid nitrogen for 15 min. 90 mL of methanol pre-cooled at  $-80\text{ }^{\circ}\text{C}$  was added into the bottle, which was kept in a refrigerator at the same temperature for 5 days. The solidified polymer was then washed with methanol several times and finally dried under vacuum at room temperature. The other polymer solutions were converted to the corresponding mesoporous materials by choosing suitable solvent systems. Cross-sectional SEM images of the nanofibre networks are shown in Fig. 1.

In our fabrication scheme, the temperature of frozen polymer solution is raised to  $-80\text{ }^{\circ}\text{C}$ . During this process, the solvent molecules start to form nanocrystals among the polymer chains. The frozen solution then separates to a polymer-rich phase and a solvent nanocrystal phase. When the polymer concentration is

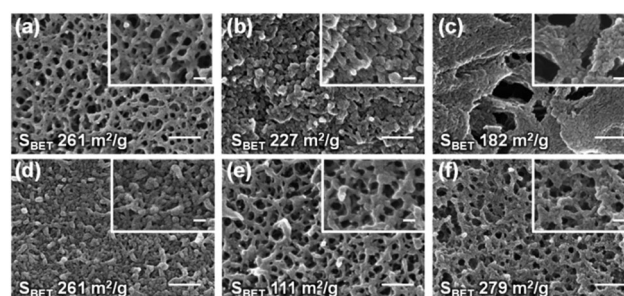


Fig. 1 SEM images of polymer nanofibre networks. (a) Polystyrene, (b) polysulfone, (c) polycarbonate, (d) polyethersulfone, (e) poly(*p*-phenylene oxide) and (f) polyetherimide. The scale bars are 200 nm (inset: 50 nm).

<sup>a</sup> National Institute for Materials Science (NIMS), 1-1 Namiki, Tsukuba, Ibaraki 305-0044, Japan. E-mail: ICHINOSE.Izumi@nims.go.jp; Fax: +81-29-852-7449; Tel: +81-29-851-3354

<sup>b</sup> Japan Science and Technology Agency, Core Research for Evolutional Science and Technology, 7 Gobancho, Chiyoda-ku, Tokyo 102-0076, Japan

† Electronic supplementary information (ESI) available: Synthesis and characterization data, detailed information on adsorption equilibrium and thermodynamic characterization. See DOI: 10.1039/c4cc01786b

increased, the rigidity of the polymer-rich phase increases rapidly. This restricts the growth of the solvent nanocrystals to the larger ones. In the appropriate range of polymer concentration, the two phases form a bicontinuous structure. Slow replacement of the nanocrystals with pre-cooled methanol leaves behind the ultrafine nanofibre network of the polymer. The specific surface area calculated from the BET plots was as high as  $261 \text{ m}^2 \text{ g}^{-1}$  for the PS nanofibre network, and the average nanofibre diameter was 16 nm. Under our experimental conditions, the thickness of sheet-shaped samples was 0.60 to 0.75 mm.

In general, the mesopores of polymer nanofibre networks are hydrophobic. However, apart from PEI, which dissolved slowly in strong acid, the inner surfaces were successfully converted to hydrophobic surfaces by means of various sulfonation techniques (see ESI†).<sup>18</sup> In the case of the PS nanofibre network, mild sulfonation with  $\text{H}_2\text{SO}_4$  was the most suitable method for controlling the hydrophilicity. To ensure complete introduction of viscous  $\text{H}_2\text{SO}_4$  into the mesopores, 1 g of the nanofibre network was immersed for 10–15 min in ethanol, and then 5 mL of conc.  $\text{H}_2\text{SO}_4$  was added. After a certain period of time, the nanofibre network was washed with methanol and deionized water. As shown in Fig. 2a, ion exchange capacities (IEC) in the range  $0.011\text{--}0.063 \text{ meq g}^{-1}$  were obtained in the sulfonated samples by choosing the reaction time and temperature (see Table S1, ESI†). After sulfonation, the PS nanofibre network shrank slightly and the specific surface area decreased to  $178 \text{ m}^2 \text{ g}^{-1}$  (Fig. 2b). However, surface modification with  $\text{H}_2\text{SO}_4$  was suitable for retention of the nanomorphology. The initial sulfonation reaction was successfully monitored based on the increase of the

FT-IR peak attributed to in-plane deformation of the sulfonated benzene ring ( $\nu_2$  in Fig. 2c).<sup>19</sup> We also confirmed the uniform sulfonation of the nanofibre network based on cross-sectional photographs of the sheet samples after staining with water-soluble dyes.

When the IEC value was  $0.011 \text{ meq g}^{-1}$ , the surface density of the sulfonated phenyl groups was calculated to be  $0.037 \text{ per nm}^2$  (or one per  $5.2 \times 5.2 \text{ nm}^2$ ). Even for the highest value ( $0.063 \text{ meq g}^{-1}$ ), the density was no more than  $0.22 \text{ per nm}^2$ . The sulfonation rate was extremely slow. This was probably because of the decreasing concentration of  $\text{H}_2\text{SO}_4$  due to the presence of ethanol in the mesopores.<sup>20</sup> Under our experimental conditions, the insides of PS nanofibres were not damaged by the sulfonation reaction, and the small number of sulfonated sites significantly improved the affinity of the nanofibres with aqueous solutions.

Fig. 2d shows the change in the UV-vis absorption spectrum of  $0.01 \text{ mM}$  methylene blue (MB) solution after immersion of the sulfonated PS nanofibre network. The  $0.7 \text{ mm}$ -thick sheet (IEC:  $0.011 \text{ meq g}^{-1}$ ,  $100 \text{ mg}$ ) removed more than 98% of the dye within 30 min. To evaluate the hydrophobic binding of the dye to the PS nanofibre network, we examined the adsorption from a  $1.0 \text{ mM}$  MB solution at pH 2.0. At this pH, the phenyl sulfonic acid groups do not dissociate and MB has a positive charge.<sup>21</sup> Using  $100 \text{ mg}$  of the sulfonated PS nanofibre network, 66% of the MB was removed after 48 h. The adsorption was not very fast, but interestingly, the mesoporous sheet was able to capture an amount of MB that was about three times greater than the number of sulfonated phenyl groups on the nanofibre surface. This indicates that there are three MB binding sites in an area of  $5.2 \times 5.2 \text{ nm}^2$ . The PS nanofibre surface is a strong adsorbent for this water-soluble dye. The enhanced mobility of the polymer chains at the nanofibre surface probably allows the formation of abundant hydrophobic binding sites.<sup>17</sup> The concentrated MB molecules on the nanofibre surfaces may associate with each other, since the association constant is no less than  $2 \times 10^3 \text{ L mol}^{-1}$ .<sup>22</sup>

A sulfonated PS nanofibre network of  $0.011 \text{ meq g}^{-1}$  was examined in detail as an adsorbent for the removal of aromatic compounds dissolved in water. Equilibrium adsorption experiments were conducted for phenol, *m*-cresol, pyridine, and aniline at temperatures of  $30 \text{ }^\circ\text{C}$ ,  $40 \text{ }^\circ\text{C}$ , and  $50 \text{ }^\circ\text{C}$  using the sheet-shaped samples. First, the equilibrium adsorption amount ( $q_e$ ,  $\text{mg g}^{-1}$ ) was calculated from the decrease in concentration of the adsorbate in solution and the values were plotted against the equilibrium concentration  $C_e$  ( $\text{mg L}^{-1}$ ) (Fig. S1, ESI†). The equilibrium isotherms were then analysed using a Freundlich equation (eqn (1)) (Fig. S2, ESI†):<sup>23</sup>

$$\ln q_e = \ln K_f + 1/n \ln C_e \quad (1)$$

where  $n$  and  $K_f$  represent the adsorption intensity and adsorption capacity. As shown in Table 1, the  $K_f$  values decreased at high temperature. The  $n$  values also decreased slightly with increasing temperature, indicating strong adsorption at low temperature. The latter values were almost equal to those of macroporous polymers<sup>24</sup> and about one-fifth of those of activated carbons.<sup>25</sup> The isosteric heat of adsorption was calculated

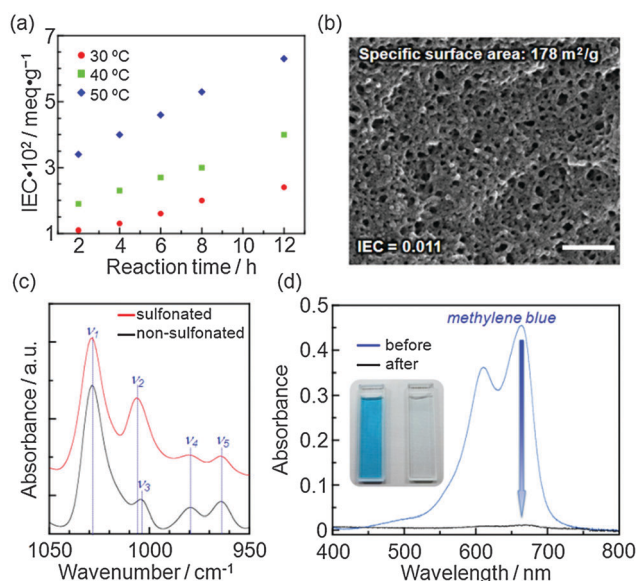


Fig. 2 (a) Increase in ion exchange capacity (ICE) with reaction time. (b) Cross-sectional SEM image of sulfonated PS nanofibre networks. The scale bar is 200 nm. The image before sulfonation is shown in Fig. 1a. (c) FT-IR spectra of PS and sulfonated-PS nanofibre networks ( $30 \text{ }^\circ\text{C}$ , 2 h). (d) UV-vis absorption spectra of methylene blue (MB) solution (5 mL) before and after treatment with the sulfonated PS nanofibre network. Initial concentration:  $0.01 \text{ mM}$  (pH 7.0). The inset shows a photographic image of the solutions.

**Table 1** Adsorption enthalpy at given equilibrium adsorption amounts and Freundlich parameters at given temperatures

| Aromatic compound | $q_e$<br>(mg g <sup>-1</sup> ) | $\Delta H$<br>(kJ mol <sup>-1</sup> ) | $T$ (K) | Freundlich parameters |       |       |
|-------------------|--------------------------------|---------------------------------------|---------|-----------------------|-------|-------|
|                   |                                |                                       |         | $n$                   | $K_f$ | $R^2$ |
| Phenol            | 2.0                            | -25.9                                 |         |                       |       |       |
|                   | 4.0                            | -21.2                                 | 303     | 1.20                  | 0.063 | 0.99  |
|                   | 6.0                            | -19.6                                 | 313     | 1.12                  | 0.039 | 0.98  |
|                   | 8.0                            | -18.5                                 | 323     | 1.11                  | 0.023 | 0.99  |
| <i>m</i> -Cresol  | 2.0                            | -42.4                                 |         |                       |       |       |
|                   | 4.0                            | -35.8                                 | 303     | 1.36                  | 0.212 | 0.99  |
|                   | 6.0                            | -30.6                                 | 313     | 1.33                  | 0.133 | 0.99  |
|                   | 8.0                            | -27.1                                 | 323     | 1.28                  | 0.092 | 0.97  |
| Pyridine          | 1.0                            | -32.2                                 |         |                       |       |       |
|                   | 1.5                            | -29.8                                 | 303     | 1.81                  | 0.140 | 0.97  |
|                   | 2.0                            | -28.2                                 | 313     | 1.69                  | 0.095 | 0.99  |
|                   | 2.5                            | -25.9                                 | 323     | 1.63                  | 0.055 | 0.99  |
| Aniline           | 1.0                            | -33.0                                 |         |                       |       |       |
|                   | 2.0                            | -33.1                                 | 303     | 1.72                  | 0.192 | 0.99  |
|                   | 3.0                            | -32.5                                 | 313     | 1.61                  | 0.124 | 0.99  |
|                   | 4.0                            | -31.6                                 | 323     | 1.53                  | 0.081 | 0.98  |

from the van't Hoff equation, which is expressed as follows (eqn (2)):<sup>26</sup>

$$\ln C_e = \left( \frac{\Delta H}{RT} \right) + \ln K_f \quad (2)$$

The enthalpy change ( $\Delta H$ ) was calculated from the slope of the plot of  $\ln C_e$  against  $1/T$  (Fig. S3, ESI†) at equivalent adsorption amounts of 2.0, 4.0, 6.0, and 8.0 mg g<sup>-1</sup>. The results are also listed in Table 1. The obtained  $\Delta H$  values were all negative, indicating that the adsorption process is exothermic. The values range between -18 and -43 kJ mol<sup>-1</sup>. Although it is necessary to consider the hydration energy of these adsorbates, the overall isosteric heat caused by the adsorption does not seem to be very strong as physical binding energy. The adsorption kinetics of these aromatic compounds were analysed using a pseudo-second-order kinetics model (eqn (3)),<sup>26</sup>

$$\frac{t}{q_t} = \frac{1}{k_2 q_{ke}^2} + \frac{1}{q_{ke}} t \quad (3)$$

The squared correlation coefficient ( $R^2$ ) of the  $t/q_t$ - $t$  plot (Fig. S4, ESI†) was no less than 0.99 and the equilibrium adsorption ( $q_{ke}$ ) calculated from the slope was fairly consistent with the  $q_e$  values obtained from the adsorption isotherms (Table 2). In contrast, when the  $q_t$  values (adsorption amount at time  $t$ ) were analysed using a pseudo-first-order model (Lagergren kinetic model), there were large deviations in the plot, and the  $R^2$  values were no more than 0.8. This indicates that the adsorption process is not ruled by a simple diffusion process.<sup>26,27</sup> The strong correlations in the pseudo-second-order kinetics model support the contention that these aromatic compounds are trapped by polymer chains and migrate *via* a hopping process among open adsorption sites. The second order rate constant ( $k_2$ ) of phenol at 30 °C was 0.081 g mg<sup>-1</sup> min, which was about twice the value observed for activated carbons.<sup>26</sup> Interestingly, the rate constant tended to increase suddenly with temperature.

**Table 2** Second-order adsorption kinetics of aromatic compounds

| Aromatic compound | $T$ (K) | Rate constant,<br>$k_2$ (g mg <sup>-1</sup> min <sup>-1</sup> ) | Equilibrium adsorption (mg g <sup>-1</sup> ) |       |       |
|-------------------|---------|---|--|-------|-------|
|                   |         |   | $q_{ke}$                                     | $q_e$ | $R^2$ |
| Phenol            | 303     | 0.081   | 1.42   | 1.30  | 0.99  |
|                   | 313     | 0.088   | 1.17   | 1.18  | 0.99  |
|                   | 323     | 0.123   | 1.13   | 0.92  | 0.99  |
| <i>m</i> -Cresol  | 303     | 0.048   | 1.75   | 1.70  | 0.99  |
|                   | 313     | 0.052   | 1.78   | 1.60  | 0.99  |
|                   | 323     | 0.222   | 1.66   | 1.48  | 0.99  |
| Pyridine          | 303     | 0.095   | 1.06   | 1.08  | 0.99  |
|                   | 313     | 0.176   | 1.01   | 1.04  | 0.99  |
|                   | 323     | 0.570   | 0.73   | 0.60  | 0.99  |
| Aniline           | 303     | 0.052   | 1.61   | 1.26  | 0.99  |
|                   | 313     | 0.200   | 1.36   | 1.16  | 0.99  |
|                   | 323     | 0.400   | 1.17   | 1.00  | 0.99  |

For instance, the  $k_2$  value of pyridine adsorption was 0.57 g mg<sup>-1</sup> min at 50 °C. This tendency is consistent with the decrease in the binding energy between the polymer chains and the adsorbates at high temperature.

In summary, the PS nanofibre network was successfully modified with sulfonate groups without disrupting the mesoporous structure. The small number of surface sulfonate groups, with an average distance of about 5 nm, significantly improved the hydrophilicity of the mesopores, leading to rapid adsorption of water-soluble dyes and aromatic compounds in water. Mesopores in particular are suitable for quick and efficient adsorption of large organic molecules. The adsorption intensities of small aromatic compounds decreased with increasing temperature, which was completely the opposite tendency to that of activated carbons.<sup>26</sup> In general, the hydration energy decreases at high temperature and the binding state of the adsorbate is stabilised in relative terms. However, the energy loss of hydration seems to be smaller than the energy loss due to the spatial fluctuation of the binding sites among polymer chains at high temperature. Mesoporous polymer nanofibre networks are expected to be applicable to the purification of oily water, since they capture water-soluble oil components and release the components at high temperatures.<sup>17</sup> This paper demonstrates the scientific grounds for temperature-dependent adsorption of aromatic compounds in water.

## Notes and references

- 1 *Porous Polymers*, ed. M. S. Silverstein, N. R. Cameron and M. A. Hillmyer, John Wiley & Sons, 2011.
- 2 K. A. Cychosz, A. G. Wong-Foy and A. J. Matzger, *J. Am. Chem. Soc.*, 2008, **130**, 6938.
- 3 R. Dawson, A. I. Cooper and D. J. Adams, *Prog. Polym. Sci.*, 2012, **37**, 530.
- 4 P. Kaur, J. T. Hupp and S. T. Nguyen, *ACS Catal.*, 2011, **1**, 819.
- 5 M. A. Hillmyer, *Adv. Polym. Sci.*, 2005, **190**, 137.
- 6 J.-S. Lee, A. Hirao and S. Nakahama, *Macromolecules*, 1988, **21**, 276.
- 7 H. Uehara, *et al.*, *Macromolecules*, 2006, **39**, 3971.
- 8 M. Seo and M. A. Hillmyer, *Science*, 2012, **336**, 1422.
- 9 K.-V. Peinemann, V. Abetz and P. F. W. Simon, *Nat. Mater.*, 2007, **6**, 992.
- 10 B. Krause, H. J. P. Sijbesma, P. Mönklü, N. F. A. van der Vegt and M. Wessling, *Macromolecules*, 2001, **34**, 8792.

- 11 E. Kiran, *J. Supercrit. Fluids*, 2009, **47**, 466.
- 12 J. H. Aubert and R. L. Clough, *Polymer*, 1985, **26**, 2047.
- 13 J. T. McCann, M. Marquez and Y. Xia, *J. Am. Chem. Soc.*, 2006, **128**, 1436.
- 14 X. Sun, T. Fujimoto and H. Uyama, *Polym. J.*, 2013, **45**, 1101.
- 15 S. Loeb and S. Sourirajan, *Advances in Chemistry*, 1963, vol. 38, p. 117.
- 16 A. J. Castro, *US Pat.*, 4,247,498/1981.
- 17 S. Samitsu, R. Zhang, X. Peng, M. R. Krishnan, Y. Fujii and I. Ichinose, *Nat. Commun.*, 2013, **4**, 2653.
- 18 F. Kucera and J. Jancar, *Polym. Eng. Sci.*, 1998, **38**, 783.
- 19 P. Atorngitjawat and J. Runt, *Macromolecules*, 2007, **40**, 991.
- 20 H. W. Gibson and F. C. Bailey, *Macromolecules*, 1980, **13**, 34.
- 21 A. K. Ghosh, *J. Am. Chem. Soc.*, 1970, **92**, 6415.
- 22 A. K. Ghosh and P. Mukerjee, *J. Am. Chem. Soc.*, 1970, **92**, 6408.
- 23 H. M. F. Freundlich, *Z. Phys. Chem.*, 1906, **57**, 385.
- 24 H. Li, M. Xu, Z. Shi and B. He, *J. Colloid Interface Sci.*, 2004, **271**, 47.
- 25 H. Hindarso, S. Ismadji, F. Wicaksana, Mudjijati and N. Indraswati, *J. Chem. Eng. Data*, 2001, **46**, 788.
- 26 V. C. Srivastava, M. M. Swamy, I. D. Mall, B. Prasad and I. M. Mishra, *Colloids Surf., A*, 2006, **272**, 89.
- 27 D. Mohan, K. P. Singh, S. Sinha and D. Ghosh, *Carbon*, 2004, **42**, 2409.